

Time-resolved characterization of *Hohlraum* radiation temperature via interferometer measurement of quartz shock velocity

R. E. Olson

Sandia National Laboratories, Albuquerque, New Mexico 87185

D. K. Bradley

Lawrence Livermore National Laboratory, Livermore, California 94551

G. A. Rochau

Sandia National Laboratories, Albuquerque, New Mexico 87185

G. W. Collins

Lawrence Livermore National Laboratory, Livermore, California 94551

R. J. Leeper

Sandia National Laboratories, Albuquerque, New Mexico 87185

L. J. Suter

Lawrence Livermore National Laboratory, Livermore, California 94551

(Received 7 May 2006; presented on 8 May 2006; accepted 6 July 2006; published online 19 October 2006)

A new technique for time-resolved measurement of *Hohlraum* radiation temperature has been successfully tested in *Hohlraums* with radiation temperatures in the range of 90–170 eV. In these experiments, *Hohlraum* radiation fields produced ablatively driven shock waves in quartz samples. A line-imaging velocity interferometer was used to track the quartz shock velocity as a function of time, and an empirical relationship (determined in these experiments) was used to relate the measured shock velocity to the *Hohlraum* radiation temperature. The test experiments were performed at the Omega facility [J. M. Soures *et al.*, Phys. Plasmas **3**, 2108 (1996)] at the University of Rochester Laboratory for Laser Energetics. The technique should also be useful for *Hohlraum* temperature measurements at other DOE/NNSA high energy density experimental facilities, such as the Z facility [R. B. Spielman *et al.*, Phys. Plasmas **5**, 2105 (1998)] at Sandia National Laboratories and the National Ignition Facility [E. I. Moses, Fusion Sci. Technol. **44**, 11 (2003)] at Lawrence Livermore National Laboratory. © 2006 American Institute of Physics. [DOI: [10.1063/1.2336458](https://doi.org/10.1063/1.2336458)]

INTRODUCTION

Two techniques have been commonly used for the measurement of *Hohlraum* radiation temperature. One technique (often referred to as “Dante”)¹ utilizes an array of *K*- and *L*-edge filtered photocathodes to view the interior *Hohlraum* wall through an aperture to measure the reradiated x-ray flux. A second technique² utilizes a streak camera detection of either the thermal luminescence or the reflectivity drop (using an active laser probe) that occurs when a strong, x-ray ablation-driven shock wave breaks through the surface of a well-characterized opaque material (usually aluminum). These two temperature measurement techniques have been used extensively in both laser-driven *Hohlraum* experiments^{3–5} and z-pinch-driven *Hohlraum* experiments.^{6–8}

The Dante measurement has the advantages of being time and spectrally resolved but suffers from a limited view factor that is not generally representative of the entire field of view seen by an inertial confinement fusion (ICF) capsule placed in the center of the *Hohlraum* or by an experimental package placed on the interior wall of the *Hohlraum*. For this reason, calculated view factor corrections⁹ must usually be applied to a Dante measurement in order to understand the drive conditions in the experiment.

The measurement of the time at which an x-ray driven shock wave emerges from the rear surface of an opaque material has the advantage of sampling the entire *Hohlraum* field of view but suffers from the fact that only a single point in time can be recorded for a particular position on the *Hohlraum* wall. Thus, an aluminum witness plate is usually machined with a series of steps or a wedge along the imaging direction of the streak camera, and the measured shock breakout times are used to determine a shock velocity. This shock velocity can be used to infer the *Hohlraum* temperature provided that the x-ray flux does not vary significantly along the length of the steps or wedge. To some extent, this temperature measurement must represent an average over a particular length of the *Hohlraum* wall. Furthermore, if the time required for the shock to penetrate the aluminum thickness exceeds the time scale of the laser or z-pinch drive pulse, this technique will only provide an indication of the peak radiation temperature achieved in the *Hohlraum*.

The new *Hohlraum* temperature measurement technique described here utilizes a line-imaging velocity interferometer¹⁰ to provide a time-resolved recording of the x-ray driven shock wave velocity within the interior of an optically transparent material (such as quartz). This tech-

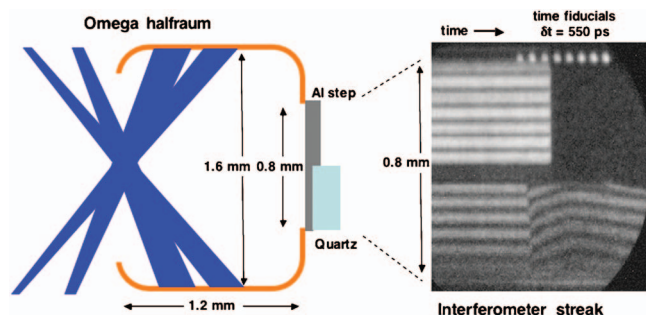


FIG. 1. (Color) The Omega halfraum experimental arrangement and a typical streaked image of the interferometer fringe pattern. Shock breakout at the Al/vacuum interface is in upper half of the streak. Shock breakout at the Al/quartz interface followed by reflection from the shock front within the quartz is in the lower half of the streak.

nique has the combined advantages of time resolution and full view of the x-ray field in the *Hohlraum* interior. In addition, it can provide time-resolved measurement of the spatial variation of the x-ray drive along the length of the interior *Hohlraum* wall. The test experiments described here were performed at the Omega laser¹¹ at the University of Rochester. The technique should also be useful for *Hohlraum* temperature measurements at other DOE/NNSA high energy density experimental facilities, such as the National Ignition Facility¹² at Lawrence Livermore National Laboratory (LLNL) and the Z facility¹³ at Sandia National Laboratories (SNL).

EXPERIMENTAL ARRANGEMENT AND DIAGNOSTIC MEASUREMENTS

The Omega experimental arrangement is depicted in Fig. 1. The cylindrical *Hohlraums* were 1.6 mm in diameter, 1.2 mm long, with a 25 μm thick Au wall, and a single 1.2 mm diameter laser entrance hole (LEH). This type of *Hohlraum* is often referred to as a “halfraum,” since there is only one LEH and it resembles half of a standard cylindrical *Hohlraum*. A quartz sample (or combined aluminum/quartz sample) was placed over a 0.80 mm diameter hole on the end of the halfraum opposite the LEH. One-fourth of the 60 Omega laser beams were used as the power source for the halfraum radiation field. In these experiments, the 15 drive beams provided a total 350 nm laser input energy in the range of 1–6 kJ with pulse shapes of either 2.0 or 3.7 ns in duration. The soft x-ray flux emitted by the hot *Hohlraum* walls (radiation temperature ~ 90 –170 eV) was absorbed in the samples and set up high pressure (~ 5 –50 Mbars) shock waves within the samples. In some of the experiments, a 120 μm thick quartz sample was positioned on the thin (25 μm) half of an aluminum step—exactly as depicted in Fig. 1. In other experiments, the quartz was positioned on the thick (50 μm) half of the step, or directly over the hole (i.e., no Al step) with only an extremely thin coating of aluminum on the interior surface of the quartz for purposes of aligning the laser and setting up the initial interferometer fringe pattern.

The layout and operation of the Omega line-imaging velocity interferometer diagnostic is described in detail in Ref. 10. In the present experiments, the 532 nm probe laser

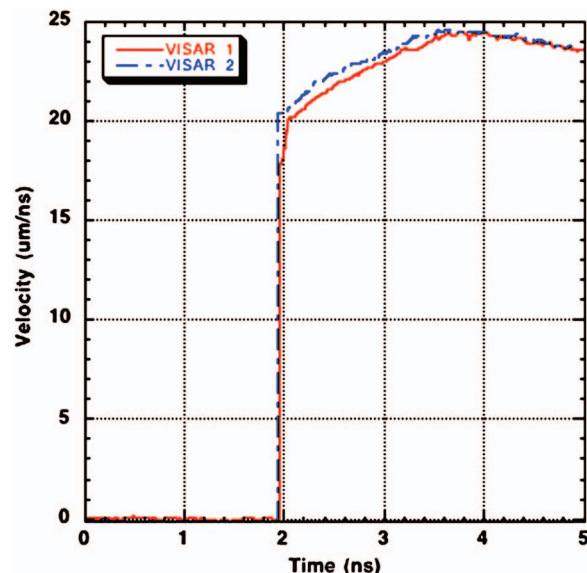


FIG. 2. (Color) Velocity-time unfolds of dual interferometer fringe patterns with two different velocity per fringe optical delay settings.

light was reflected from the shock front within the quartz, and the return signal was split and propagated through two independent interferometers (with different optical delays to provide different velocity per fringe sensitivities) and imaged onto the slits of two optical streak cameras. Each of the resulting streaked images contains a series of Doppler-shifted fringes, whose phase is directly proportional to the velocity of the reflecting shock front surface (as explained in Refs. 10 and 14–16). The streaked interferograms recorded in these experiments were reduced to time-resolved velocities using the procedures described in Ref. 10. As in that discussion, the dual interferometer data sets were used to obtain a unique determination of the Doppler shift and resulting shock front velocity (Fig. 2). In some experiments, three additional verifications of the velocity were available. First, since the quartz thickness is known, time integration of the interferometer-determined shock velocity can be used to verify that the unfold is in agreement with the shock transit time indicated by the streak camera image [Fig. 3(a)]. Second, in experiments having an aluminum step, the shock velocity in the aluminum can be determined from the streaked image and used to verify that the fringe ambiguities have been resolved correctly in the dual interferometer unfolds. As a third check, we also ran an absolutely calibrated streaked optical pyrometer¹⁷ (SOP) in line with the Omega interferometer diagnostic. This diagnostic provided independent verification of the time-averaged shock velocities in the aluminum step and the quartz sample [Fig. 3(b)]. In addition, the SOP was used in some experiments to verify that the time-resolved quartz shock front temperature was consistent with time-resolved shock velocity unfold.

CALIBRATION OF QUARTZ SHOCK VELOCITY AS A HOHLRAUM RADIATION TEMPERATURE DIAGNOSTIC

The Omega Dante diagnostic was used in these test and calibration experiments to provide an independent time-

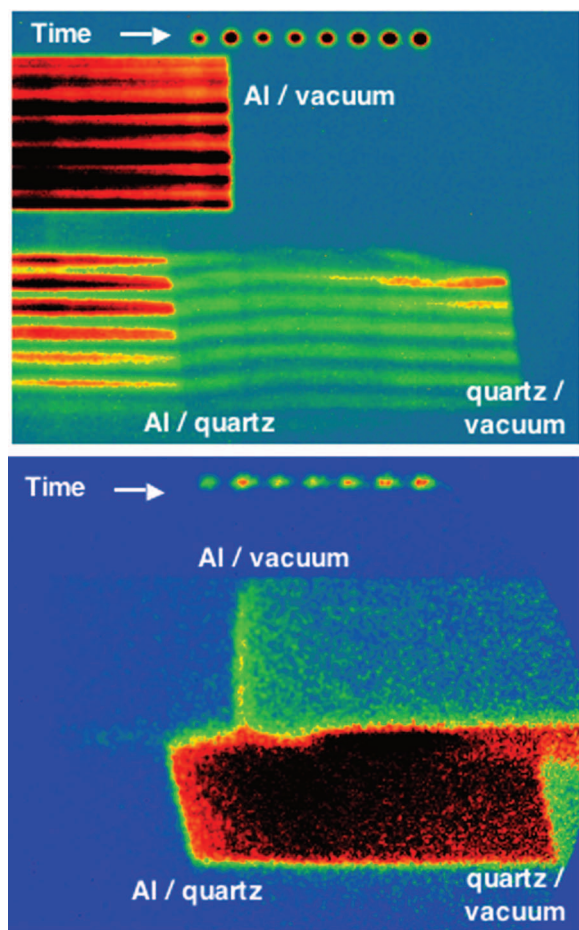


FIG. 3. (Color) (a) The upper image is an interferometer streak in which the transit times for shock propagation across the aluminum step and the quartz sample are clearly discernible. (b) The lower image is a SOP streak (of the same experiment) in which the shock thermal luminescence can be used to verify the shock transit times. In both images, the time fiducials are at 550 ps intervals.

resolved temperature measurement (the interior halfraum wall was viewed through the LEH). The Dante unfolds were

performed at SNL using filter, photocathode, and grazing-incidence mirror calibrations supplied by LLNL and an unfold routine based upon the iterative deconvolution procedure described in Ref. 3. Dante temperature history unfolds for experiments with *Hohlraum* temperatures T covering the range of 90–170 eV are shown in Fig. 4(a). Interferometer measurements of the quartz shock velocities for these same experiments are shown in Fig. 4(b).

Since the x-ray flux absorbed by the quartz surface (or aluminum surface in the experiments employing the Al step) is proportional to T^4 and the ablation velocity is proportional to $T^{0.5}$, it follows that the indirect-drive ablation pressure ought to be proportional to $T^{3.5}$. Furthermore, since the shock pressure is proportional to the product of the shock velocity (v_s) and particle velocity and the particle velocity is approximately linearly related to the shock velocity (to within 1.5% for quartz¹⁸ in the range of interest for these experiments), it follows that the shock pressure ought to be proportional to v_s^2 . If the ablation pressure and shock pressure are equated, it then follows that the *Hohlraum* temperature is proportional to $v_s^{0.57}$. The constant of proportionality would be expected to depend in detail upon such things as the ionization state and albedo of the ablation material but (for aluminum or quartz) ought to vary only slightly over the temperature range of these experiments. Application of this reasoning to the plots shown in Fig. 4 results in the overlay plot shown in Fig. 5(a), where it is empirically determined that the appropriate scaling for this temperature range is T (eV) = $21.4v_s^{0.57}(\mu\text{m/ns})$. Inspection of Fig. 5(a) leads to the somewhat obvious conclusion that a time shift (between the Dante and interferometer unfolds) must be included in order to obtain an exact correspondence of the temperature-time plots. Radiation-hydrodynamic computer simulations were used to confirm the speculation that the time delay is inversely proportional to the shock velocity. An empirical scaling that fits the data is $t_{\text{shift}}(\text{ns}) = 12.0/v_s(\mu\text{m/ns})$. This time shift has been applied in Fig. 5(b), in which data from an

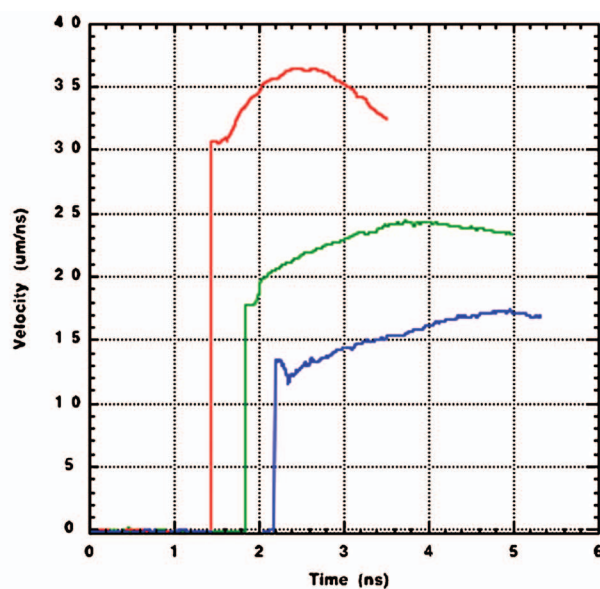
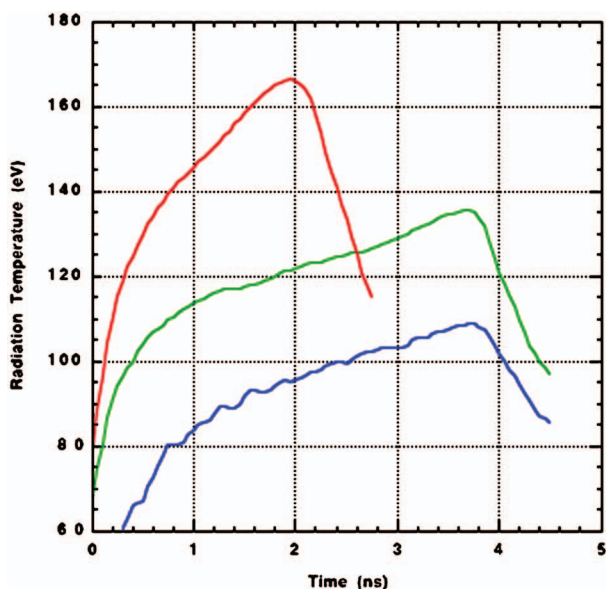


FIG. 4. (Color) (a) Dante temperature history unfolds for experiments with *Hohlraum* temperatures T covering the range of 90–170 eV. (b) Interferometer measurements of the quartz shock velocities for these same experiments.

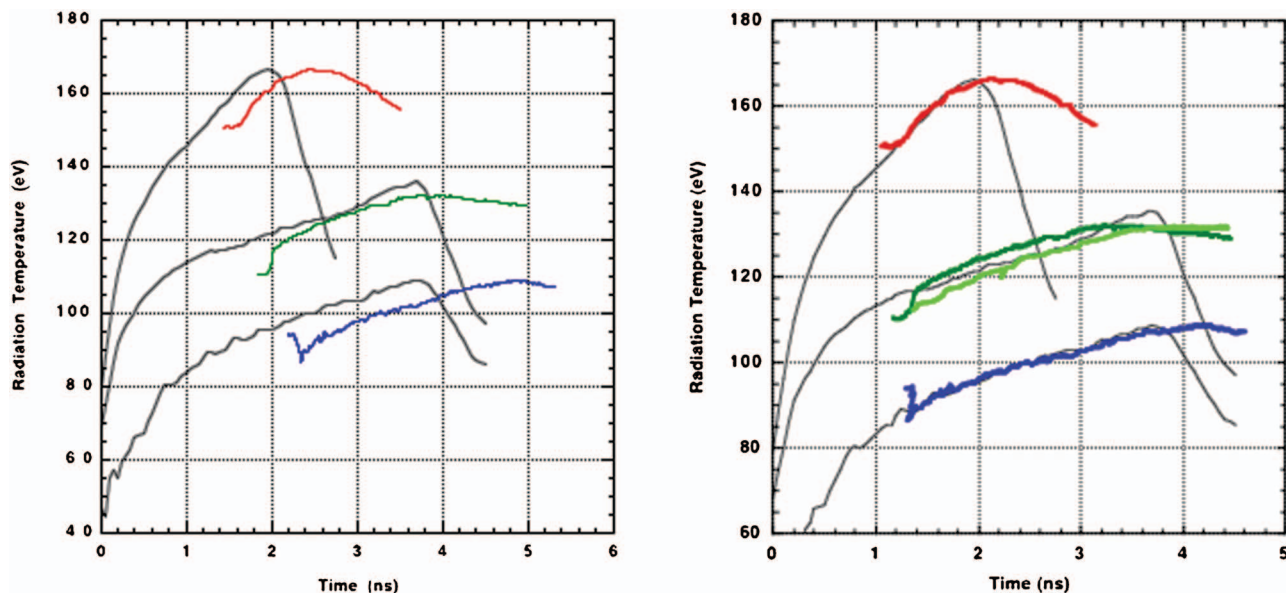


FIG. 5. (Color) (a) The empirical scaling $T \text{ (eV)} = 21.4v_s^{0.57} \text{ (}\mu\text{m/ns)}$ has been applied to the velocity-time plots shown in Fig. 4(b) and then overlaid on the Dante $T(t)$ plots of Fig. 4(a). The time shift correction $t_{\text{shift}} \text{ (ns)} = 12.0/v_s \text{ (}\mu\text{m/ns)}$ has been applied to the velocity interferometer-determined temperatures and then overlaid on the Dante $T(t)$ plots. The additional plot covering the midrange temperatures is from an experiment in which only the quartz component was used (i.e., no aluminum step).

additional experiment are added to indicate the slight differences that may exist when using this measurement technique with and without the aluminum component.

PREHEAT LIMITATIONS

For the situation of a truly Planckian *Hohlraum* radiation temperature, essentially all of the x rays will be absorbed at the ablation front, and a *Hohlraum* temperature can be accurately determined from a shock velocity measurement. Unfortunately, for the case of a laser *Hohlraum*, there is a limitation due to the non-Planckian aspects of the radiation field. Although the majority of the laser *Hohlraum* x-ray flux is absorbed at the ablation front and contributes to the drive of the shock wave, there will be a significant component of hard ($>1.5 \text{ keV}$) x-ray flux (from Au *M*-band emission) that can penetrate beyond the ablation and shock fronts and can preheat material ahead of the shock front. It is well known that this preheat can be a very important aspect of laser *Hohlraum* experiments, and descriptions of the laser *Hohlraum* preheat sources and experimental measurements of the preheat effects in ablator materials have been presented in previous publications.^{19–21} In the present experiments, we find that as the *Hohlraum* temperature increases (with an increasing laser input intensity), the preheat level eventually increases to the point at which the shocked material loses its optical transparency in the region ahead of the shock. An example of this effect is shown in Fig. 6. In the present work, we have been limited by the preheat in laser *Hohlraums* with temperatures above 170 eV, with the “blank-out” effect resulting in a total loss of interferometer data for the 190 eV *hohlraums* with *M*-band flux exceeding $\sim 50 \text{ GW/sr}$.

DISCUSSION AND ONGOING WORK

In conclusion, a new technique for time-resolved measurement of *Hohlraum* temperature has been successfully

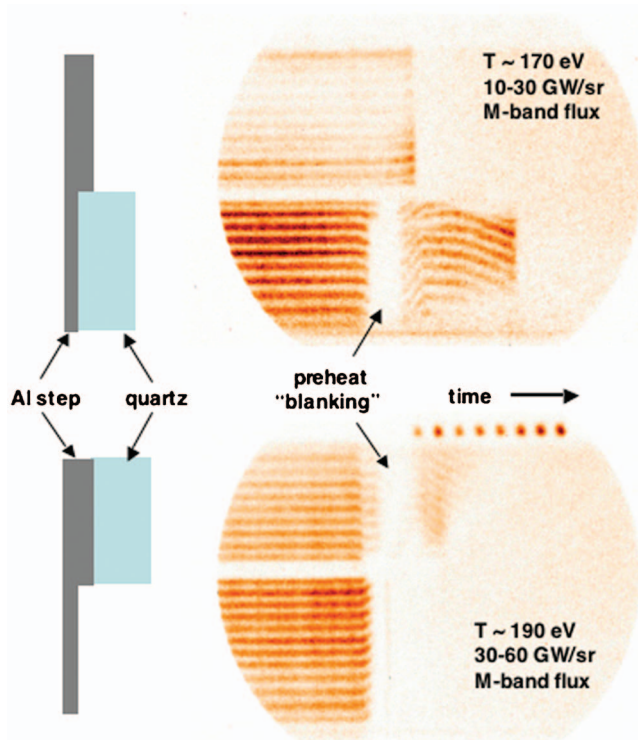


FIG. 6. (Color) As the *Hohlraum* temperature is increased (via increasing the laser input power and intensity), the problem of preheat ahead of the shock increases. This results in a loss of optical transparency in the quartz and, hence, a “blanking” of the data in the interferometer streaked image. Interestingly, it appears that the optical transparency of the quartz recovers after the end of the laser pulse (especially in the upper image).

tested for Omega laser-driven halfraums with temperatures in the range of 90–170 eV. The empirical relationship T (eV) = $21.4v_s^{0.57}$ ($\mu\text{m/ns}$) has been established to unfold a *Hohlraum* temperature from a quartz shock velocity, and the empirical relationship t_{shift} (ns) = $12.0/v_s$ ($\mu\text{m/ns}$) has been established to correct for the time delay due to shock pressure transit from the ablation front to the shock front. An important limitation for measurements in laser-driven *Hohlraums* is found to be caused by super-Planckian preheat photons when the flux of such photons exceeds ~ 50 GW/sr.

Two new initiatives have begun to extend the capabilities of this diagnostic technique. The data presented here indicate that this *Hohlraum* temperature measurement is well behaved for continuously rising temperature pulses in the range of 90–170 eV. In recent Omega halfraum experiments, the measurement technique has been extended to situations in which shaped laser pulses have been used to produce noncontinuously rising temperatures or sudden increases in the *Hohlraum* radiation field resulting in multiple shock fronts that converge within the quartz sample. A second new initiative is underway to develop this *Hohlraum* temperature measurement capability in *z*-pinch *Hohlraums* at SNL. In ongoing experiments at the Z facility, an interferometer diagnostic of the type described in Ref. 22 is being coupled via fiber optic to the surface of a quartz sample, which is, in turn, attached to a *z*-pinch-driven halfraum similar to the one described in Ref. 8. The radiation temperatures in these experiments are of the continuously rising variety and are ~ 110 – 150 eV—within the range that has been calibrated in the Omega test experiments described in the present article.

ACKNOWLEDGMENTS

The authors acknowledge helpful discussions with P. M. Celliers (LLNL), T. R. Boehly (UR/LLE), D. G. Hicks (LLNL), and B. A. Hammel (LLNL). The authors thank the

Omega laser operations and diagnostics teams for making these experiments possible. The halfraums and samples were assembled by C. Russell and the Schafer/General Atomics (GA) fabrication team at SNL. The halfraums and aluminum steps were fabricated by J. Kaae and the GA fabrication team in San Diego, CA. The quartz samples were provided by W. Unites (LLNL). K. M. Campbell (LLNL) provided the synchrotron calibrations of the Dante filters and photocathodes. Sandia is a multiprogram laboratory operated by the Sandia Corporation, a Lockheed Martin Company, for the U.S. Department of Energy under Contract No. DE-AC04-94AL85000.

- ¹H. N. Kornblum, R. L. Kauffman, and J. A. Smith, Rev. Sci. Instrum. **57**, 2179 (1986).
- ²T. Lower *et al.*, Phys. Rev. Lett. **72**, 3186 (1994).
- ³R. L. Kauffman *et al.*, Rev. Sci. Instrum. **66**, 678 (1995).
- ⁴C. Decker *et al.*, Phys. Rev. Lett. **79**, 1491 (1997).
- ⁵E. L. Dewald *et al.*, Phys. Rev. Lett. **95**, 215004 (2005).
- ⁶R. E. Olson *et al.*, Phys. Plasmas **4**, 1818 (1997).
- ⁷T. W. L. Sanford *et al.*, Phys. Rev. Lett. **83**, 5511 (1999).
- ⁸R. E. Olson *et al.*, Rev. Sci. Instrum. **72**, 1214 (2001).
- ⁹D. H. Cohen, O. L. Landen, and J. J. MacFarlane, Phys. Plasmas **12**, 122703 (2005).
- ¹⁰P. M. Celliers, D. K. Bradley, G. W. Collins, D. G. Hicks, T. R. Boehly, and W. J. Armstrong, Rev. Sci. Instrum. **75**, 4916 (2004).
- ¹¹J. M. Soures *et al.*, Phys. Plasmas **3**, 2108 (1996).
- ¹²E. I. Moses, Fusion Sci. Technol. **44**, 11 (2003).
- ¹³R. B. Spielman *et al.*, Phys. Plasmas **5**, 2105 (1998).
- ¹⁴L. Barker and R. Hollenbach, Rev. Sci. Instrum. **36**, 1617 (1965).
- ¹⁵L. Barker and R. Hollenbach, J. Appl. Phys. **41**, 4208 (1970).
- ¹⁶L. Barker and R. Hollenbach, J. Appl. Phys. **43**, 4669 (1972).
- ¹⁷J. A. Oertel *et al.*, Rev. Sci. Instrum. **70**, 803 (1999).
- ¹⁸Los Alamos National Laboratory Report NO. LA-10160-MS, SESAME 7381 edited by K. S. Holian, 1984 (unpublished).
- ¹⁹R. E. Olson, R. J. Leeper, A. Nobile, and J. A. Oertel, Phys. Rev. Lett. **91**, 235002 (2003).
- ²⁰R. E. Olson *et al.*, Phys. Plasmas **11**, 2778 (2004).
- ²¹R. E. Olson, R. J. Leeper, G. A. Rochau, D. K. Bradley, P. M. Celliers, and T. R. Boehly, J. Phys. IV **133**, 179 (2006).
- ²²M. D. Knudson, D. L. Hanson, J. E. Bailey, C. A. Hall, and J. R. Asay, Phys. Rev. Lett. **90**, 35505 (2003).